



Published in final edited form as:

ACS Sens. 2017 September 22; 2(9): 1257–1261. doi:10.1021/acssensors.7b00425.

## A Reversible Reaction-Based Fluorescent Probe for Real-Time Imaging of Glutathione Dynamics in Mitochondria

Jianwei Chen<sup>1,‡</sup>, Xiqian Jiang<sup>1,‡</sup>, Chengwei Zhang<sup>1</sup>, Kevin R. MacKenzie<sup>1,2</sup>, Fabio Stossi<sup>3,4</sup>, Timothy Palzkill<sup>1,2</sup>, Meng C. Wang<sup>5,6</sup>, and Jin Wang<sup>1,2,3,\*</sup>

<sup>1</sup>Department of Pharmacology and Chemical Biology, Baylor College of Medicine, Houston, TX 77030, USA

<sup>2</sup>Center for Drug Discovery, Baylor College of Medicine, Houston, TX 77030, USA

<sup>3</sup>Department of Molecular and Cellular Biology, Baylor College of Medicine, Houston, TX 77030, USA

<sup>4</sup>Integrated Microscopy Core, Advanced Technology Cores, Baylor College of Medicine, Houston, TX 77030, USA

<sup>5</sup>Department of Molecular and Human Genetics, Baylor College of Medicine, Houston, TX 77030, USA

<sup>6</sup>Huffington Center on Aging, Baylor College of Medicine, Houston, TX 77030, USA

### Abstract

We report a mitochondria-specific glutathione (GSH) probe—designated as Mito-RealThiol (MitoRT)—that can monitor *in vivo* real-time mitochondrial glutathione dynamics, and apply this probe to follow mitochondrial GSH dynamic changes in living cells for the first time. MitoRT can be utilized in confocal microscopy, super-resolution fluorescence imaging, and flow cytometry systems. Using MitoRT, we demonstrate that cells have a high priority to maintain the GSH level in mitochondria compared to the cytosol not only under normal growing conditions but also upon oxidative stress.

### TOC image

---

**Corresponding Author:** wangj@bcm.edu.

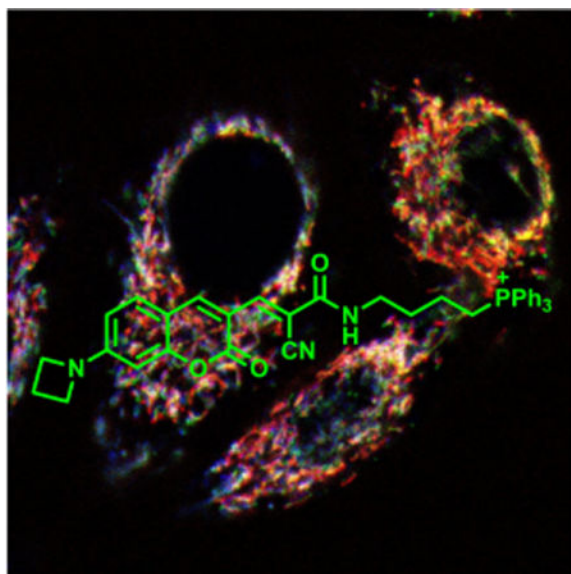
**‡Author Contributions:** These authors contributed equally.

#### Supporting Information

Chemical synthesis of MitoRT, experimental details of cell culture, confocal imaging, super-resolution imaging and flow cytometry. The Supporting Information is available free of charge on the ACS Publications website.

#### Notes

X.J., J.C. and J.W. are co-inventors of a patent application related to this work.



### Keywords

Glutathione; Mitochondria; Oxidative Stress; Sensors and Probes; Fluorescence Imaging; Flow Cytometry

Although glutathione (GSH) is exclusively synthesized in the cytosol, it distributes to intracellular organelles at different concentrations.<sup>1</sup> Mitochondria are the primary site of intracellular energy production and the major source of reactive oxygen species (ROS).<sup>2</sup> Mitochondrial GSH (mGSH) is a critical component of antioxidant defense systems to counter the potential oxidative damage generated during normal aerobic metabolism.<sup>2</sup> Therefore, a proper concentration of mGSH is crucial for maintaining the redox homeostasis in mitochondria. Biochemical assays were used to measure mGSH in isolated mitochondria from whole cell lysates and suggested the concentration of mGSH is similar to that of the cytosol (~10 mM).<sup>1,3</sup> Redox-sensitive green fluorescent proteins (roGFPs) have been widely used to measure the GSH redox potential ( $E_{\text{GSH}}$ ) in living cells.<sup>4,5</sup> Using a mitochondria-specific roGFP, Bhaskar et al. showed that the values of  $E_{\text{GSH}}$  are similar in the cytosol and mitochondria (~ -310 mV).<sup>6</sup> However, this measurement approached the detection limit of roGFP, which may underestimate the mGSH level. Additionally,  $E_{\text{GSH}}$  is proportional to  $[\text{GSH}]^2: [\text{GSSG}]$ . Changes in  $E_{\text{GSH}}$  may be due to changes of [GSH], or changes of [GSSG], or a combination of both. Therefore, to better understand the roles of mGSH and the regulation of its concentration, a new method is urgently needed to follow the dynamic changes of mGSH levels in living cells.

Although mitochondria-specific GSH probes were reported previously, all these probes are based on irreversible reactions and cannot provide any information on mGSH dynamics in living cells.<sup>7,8</sup> Our group reported the first reversible reaction-based GSH probe (ThiolQuant Green) that can perform single-point quantification of GSH levels in living cells.<sup>9,10</sup> Building on this work, we,<sup>11</sup> Urano<sup>12</sup> and Yoon<sup>13</sup> independently reported reversible reaction-based fluorescent probes that can quantitatively monitor GSH dynamics in real-

time. In our design, the RealThiol (RT) probe uniformly distributes inside cells, reversibly reacts with GSH with a dissociation equilibrium constant  $K_d$  of 3.7 mM, and responds to GSH level changes within 60 s, providing a convenient tool to monitor the global GSH levels in living cells in real-time. In this contribution, we report a mitochondria-specific GSH probe, namely Mito-RealThiol (MitoRT, Fig. 1), and apply this probe to follow mGSH dynamic changes in living cells and during different biological processes for the first time.

We designed MitoRT by substituting the carboxylic acid groups in RT with a triphenylphosphonium (TPP) group, which can preferentially target mitochondria taking advantage of the highly negative mitochondrial membrane potential (Fig. 1).<sup>14</sup> The 4-carbon linker between TPP and the Michael acceptor in MitoRT is chosen based on extensive optimization to balance the mitochondrial specificity of both MitoRT and its GSH adduct (MitoRT-GSH). In the case of a two-carbon linker, although the probe shows excellent mitochondria specificity, its GSH adduct displays diffusive distribution in cells, possibly because the negatively charged GSH neutralizes the positively charged TPP through intramolecular interactions (Supplementary Figures 1A and 1B). In contrast, with an eight-carbon linker, the probe is not readily water soluble and mostly adheres to the plasma membrane of the cell (Supplementary Figures 1A and 1C). In contrast, with a 4-carbon linker, both MitoRT and MitoRT-GSH provide optimal mitochondria specificity in living cells (Fig. 1).

MitoRT shows ratiometric fluorescence responses with a wide dynamic range when reacting with GSH. MitoRT and MitoRT-GSH show fluorescence maxima at 567 and 488 nm with excitation wavelengths at 488 and 405 nm, respectively (Fig. 2a). When MitoRT (6  $\mu$ M) equilibrates with increasing concentrations of GSH (0–80 mM), we observed the absorbance decreases at 488 nm and concurrently increases at 395 nm with an isosbestic point at 430 nm (Fig. 2b). Fitting the normalized absorbance at 405 and 488 nm using a sigmoidal function afforded the dissociation equilibrium constant  $K_d$  for the reaction between MitoRT and GSH to be 1.0 mM (Fig. 2c). The fluorescence changes of MitoRT are also GSH dose dependent (Supplementary Figure 2). Plotting the corrected fluorescence intensity ratios  $(R - R_{\min}) / (R_{\max} - R)$  as a function of GSH concentrations confers a superb linear relationship ( $R^2 = 0.991$ ) covering the physiological GSH concentration range 1–10 mM (Fig. 2d), in which  $R = F_{405} / F_{488}$ .  $F_{405}$  and  $F_{488}$  are the fluorescence intensities for RT-GSH and RT, respectively.  $R_{\min}$  and  $R_{\max}$  are the  $R$  values at 0 and saturating (80 mM) GSH concentrations, respectively. Based on Lavis's pioneering work,<sup>15</sup> we introduced an azetidine group to substitute the diethylamino group in coumarin to increase the quantum yield and photostability of the probe. The quantum yields of MitoRT and MitoRT-GSH are 0.20 and >0.97 in PBS, respectively (the quantum yield of MitoRT-GSH is greater than that of the reference rhodamine, which is 0.97). Due to both the high abundance of GSH and the millimolar  $K_d$  value, we observed  $F_{405} / F_{488}$  changes only when MitoRT reacted with GSH but not with other thiols, reactive oxygen or nitrogen species (ROS/RNS) at their corresponding physiological concentrations (Fig. 2e).

MitoRT shows fast reaction kinetics with GSH in both forward and reverse directions, enabling real-time monitoring of mGSH dynamics in living cells. To measure the forward reaction rates, we mixed MitoRT (1  $\mu$ M) with an equal volume of GSH solution (5 mM) at

pH 7.4 and monitored the formation of MitoRT-GSH using a stopped-flow mixer with fluorescence detection ( $\lambda_{\text{ex}} = 395 \text{ nm}$ ) (Fig. 2f). Unlike the pseudo first-order reaction kinetics between RT and GSH, the reaction kinetics between MitoRT and GSH are biphasic. The detailed kinetic analyses between a series of GSH probes and GSH will be reported in a follow-up study. A representative biphasic kinetic trace is shown for the reaction between MitoRT and 5 mM of GSH with  $k_{\text{fast}} = 0.51 \text{ s}^{-1}$  and  $k_{\text{slow}} = 0.042 \text{ s}^{-1}$  (Fig. 2f). With 5 mM of GSH, it takes 26.5 seconds to reach 90% of reaction completion. To measure the reverse reaction rates, we mixed a pre-equilibrated mixture of MitoRT (1  $\mu\text{M}$ ) and GSH (5 mM) with an equal volume of PBS and followed the disappearance of MitoRT-GSH fluorescence ( $\lambda_{\text{ex}} = 395 \text{ nm}$ ) (Fig. 2g). Similar to the forward reaction, the reverse reaction kinetics is also biphasic with a 90% completion time of 32.4 seconds. To further demonstrate the reversibility of the reaction between MitoRT and GSH, we sequentially added GSH to a MitoRT solution (1  $\mu\text{M}$ ) to reach final GSH concentrations of 0.5, 1.0, 2.0, and 3.0 mM, and observed step-wise establishment of equilibria by monitoring the fluorescence changes of MitoRT-GSH ( $\lambda_{\text{ex}} = 405 \text{ nm}$ ), a hall-mark of reversible reactions (Fig. 2h). We then added *N*-methylmaleimide (NMM, final concentration of 3.0 mM) to scavenge all the added GSH and observed complete recovery of MitoRT fluorescent signal, demonstrating that the reaction between MitoRT and GSH is fully reversible.

To demonstrate the mitochondria specificity of MitoRT and MitoRT-GSH in living cells, HeLa cells were incubated with MitoRT (1  $\mu\text{M}$ ) and MitoTracker Red CMXRos for 30 minutes and imaged using a confocal microscope with excitation wavelengths of 405, 488 and 595 nm. As shown in Fig. 3a, both MitoRT and MitoRT-GSH staining colocalize well with MitoTracker Red staining, demonstrating high mitochondria specificity of MitoRT and MitoRT-GSH. Quantitative colocalization analyses validate a significant correlation based on the Pearson's and Manders' coefficients (Person's coefficient = 0.74, Mander's coefficients M1 = 0.76, M2 = 0.84).<sup>16</sup> Super-resolution fluorescence microscopic imaging using structured illumination (SIM) further confirms mitochondrial morphology based on MitoRT staining (Fig. 3b).

MitoRT responds to the real-time changes of mGSH levels in living cells. For cells treated with MitoRT (1  $\mu\text{M}$  final concentration in culture medium), real-time ratiometric images reflecting mGSH levels in single cells can be generated by dividing the fluorescence intensity value from the 405 nm channel by that from the 488 nm channel at each corresponding pixel ( $F_{405 \text{ nm}}/F_{488 \text{ nm}}$ ) (Fig. 3c). It should be noted that due to the dynamic nature of mitochondria, both 405 and 488 nm lasers are required to be applied simultaneously with concurrent collection of fluorescence emissions in both channels (410–483 nm and 499–624 nm). If the fluorescence images were acquired sequentially under the two excitation wavelengths, significant image offsets could be observed, resulting in artefacts in ratiometric analyses. To monitor dynamic changes of mGSH upon oxidative stress, MitoRT stained HeLa cells were treated with a bolus addition of 100  $\mu\text{M}$  of  $\text{H}_2\text{O}_2$ . Time-lapsed confocal imaging showed a rapid decrease of fluorescence intensity in the 405 nm channel along with a concurrent increase in the 488 nm channel. The changes of the ratiometric map ( $F_{405 \text{ nm}}/F_{488 \text{ nm}}$ ) revealed a dramatic reduction of mGSH levels in mitochondria due to oxidative stress, and demonstrate the ability of MitoRT to sensitively monitor mGSH homeostasis in living cells. It should be noted that the mGSH level

recovered to the basal level after 400 seconds, presumably due to glutathione reductase activity in mitochondria (Figs. 3c and 3d), suggesting that application of MitoRT at 1  $\mu\text{M}$  level does not affect endogenous redox balance in mitochondria. Interestingly, if 500  $\mu\text{M}$  of  $\text{H}_2\text{O}_2$  was added to HeLa cells, we could not observe the recovery of mGSH level. These experiments demonstrate that MitoRT reversibly reacts with GSH inside cells and can monitor mGSH dynamics.

In addition, we applied fluorescence activated cell sorting (FACS) to demonstrate that MitoRT can be used to compare mGSH levels in living cells in a high throughput manner (Figs. 3e and 3f). Serum starvation is known to trigger oxidative stress in cells.<sup>17</sup> However, the changes of the mGSH level, if any, during serum starvation are unknown. HeLa cells were cultured in Dulbecco modified eagle medium (DMEM) with or without 10% of fetal bovine serum (FBS) for 24 h. We then stained the cells with 1  $\mu\text{M}$  of MitoRT for 15 minutes at 37 °C prior to FACS analysis. Pacific blue ( $\lambda_{\text{ex}} = 405 \text{ nm}$ ,  $\lambda_{\text{em}} = 430\text{--}470 \text{ nm}$ ) and PE channels ( $\lambda_{\text{ex}} = 488 \text{ nm}$ ,  $\lambda_{\text{em}} = 549\text{--}601 \text{ nm}$ ) were used. Ratio  $F_{405 \text{ nm}}/F_{488 \text{ nm}}$ , which is positively correlated with the mGSH levels, was calculated based on the fluorescence intensities from the two channels. As shown in Fig. 3e, FBS deprivation caused an increase of the mGSH level compared to the cells cultured with FBS. Because GSH can only be synthesized in the cytosol, the increase of mGSH level during FBS starvation must be due to GSH import from the cytosol. Interestingly, based on RT measurements, the cytosolic GSH level remains unchanged under the same FBS starvation condition (Fig. 3e). On the other hand, if sulfur containing amino acids (SCAAs) were depleted from the medium to prevent GSH synthesis, FBS starvation induced a similar increase of mGSH, but a significant decrease of cytosolic GSH. Together, these results suggest that upon serum starvation, cytosolic GSH synthesis is increased and imported into mitochondria to support the increase of mGSH. We also found that if cells were cultured in DMEM with FBS but without SCAAs to restrict GSH synthesis, mGSH maintains the same level as the cells cultured in regular DMEM with FBS, while cytosolic GSH decreases. Thus, these experiments demonstrate that cells have high priority to maintain the mGSH level compared to the cytosolic GSH level.

In summary, we have developed a fluorescent probe that enables real-time imaging of mGSH in living cells. We demonstrate that MitoRT preferentially reacts with GSH under physiological conditions and responds to both increases and decreases in GSH levels within 30 seconds. Furthermore, MitoRT has a high quantum yield, which allows minimal perturbation of the biological system by using 1  $\mu\text{M}$  of the probe. In addition, MitoRT is capable of monitoring mGSH changes upon redox perturbation, which is essential in studying mitochondria redox biology, especially fast processes, in living cells. Not only suitable for fluorescence imaging studies, MitoRT can also be conveniently applied in flow cytometry to compare mGSH levels and potentially be multiplexed with other probes and cell surface markers. Using both RT and MitoRT probes, we demonstrated that cells prioritize to maintain mGSH levels compared to the cytosolic GSH level at different growth conditions. MitoRT will be a useful tool in studying mGSH dynamics and transportation and advance our understanding of the physiological and pathological roles of mGSH in living cells.

## Supplementary Material

Refer to Web version on PubMed Central for supplementary material.

## Acknowledgments

The research was supported in part by the National Institutes of Health (R01-GM115622, R01-CA207701, R21-CA213535 to J.W., R01-AG045183, R01-AT009050, R21-EB022302, and DP1-DK113644 to M.C.W.), the Welch Foundation (Q-1912 to M.C.W.), Cancer Prevention and Research Institute of Texas (CPRIT R1104 to J.W.), the IDDRC Microscopy Core (P30HD024064 and 1U54 HD083092 Intellectual and Developmental Disabilities Research Grant from the Eunice Kennedy Shriver National Institute of Child Health and Human Development), the Optical Imaging and Vital Microscopy core, and the Cytometry and Cell Sorting Core at Baylor College of Medicine with funding from the NIH (AI036211, CA125123, and RR024574) and the expert assistance of Joel M. Sederstrom. Super-resolution imaging for this project was supported by the Integrated Microscopy Core at Baylor College of Medicine with funding from NIH (DK56338, and CA125123), CPRIT (RP150578), the Dan L. Duncan Comprehensive Cancer Center, and the John S. Dunn Gulf Coast Consortium for Chemical Genomics.

## References

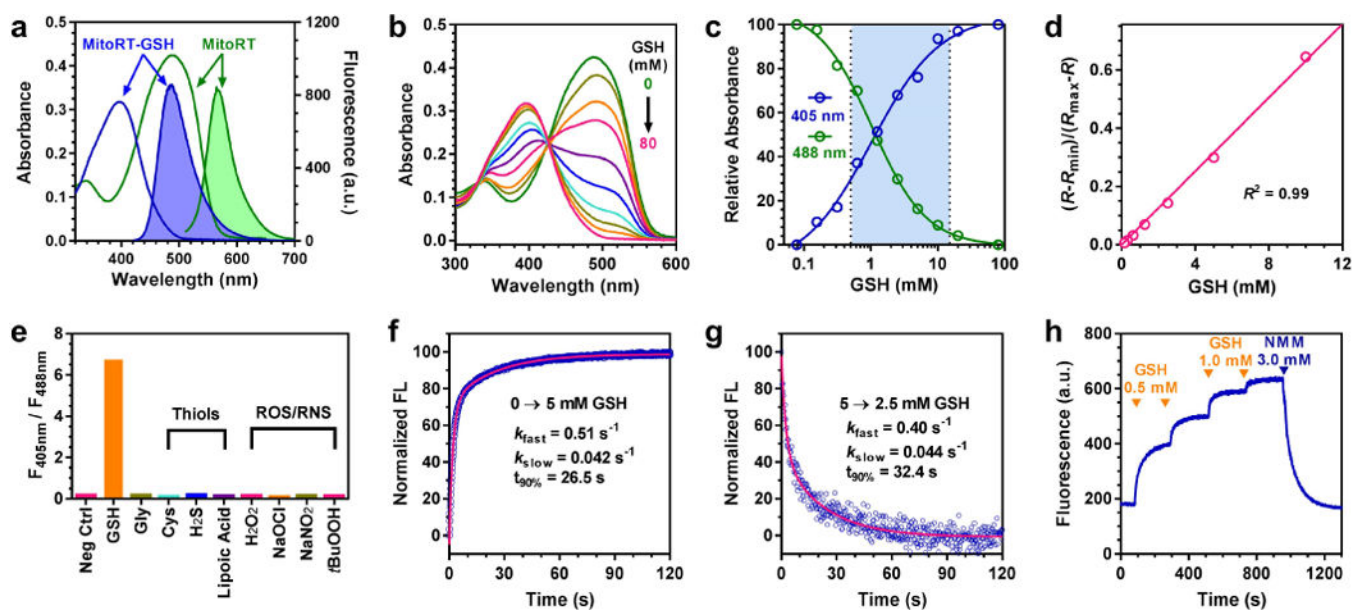
1. Mari M, Morales A, Colell A, Garcia-Ruiz C, Kaplowitz N, Fernandez-Checa JC. Mitochondrial glutathione: features, regulation and role in disease. *Biochimica et biophysica acta*. 2013; 1830:3317–3328. [PubMed: 23123815]
2. Mari M, Morales A, Colell A, Garcia-Ruiz C, Fernandez-Checa JC. Mitochondrial glutathione, a key survival antioxidant. *Antioxidants & redox signaling*. 2009; 11:2685–2700. [PubMed: 19558212]
3. Griffith OW, Meister A. Origin and turnover of mitochondrial glutathione. *Proceedings of the National Academy of Sciences of the United States of America*. 1985; 82:4668–4672. [PubMed: 3860816]
4. Gutscher M, Pauleau AL, Marty L, Brach T, Wabnitz GH, Samstag Y, Meyer AJ, Dick T. P Real-time imaging of the intracellular glutathione redox potential. *Nature methods*. 2008; 5:553–559. [PubMed: 18469822]
5. Hanson GT, Aggeler R, Oglesbee D, Cannon M, Capaldi RA, Tsien RY, Remington S. J Investigating mitochondrial redox potential with redox-sensitive green fluorescent protein indicators. *The Journal of biological chemistry*. 2004; 279:13044–13053. [PubMed: 14722062]
6. Bhaskar A, Munshi M, Khan SZ, Fatima S, Arya R, Jameel S, Singh A. Measuring glutathione redox potential of HIV-1-infected macrophages. *The Journal of biological chemistry*. 2015; 290:1020–1038. [PubMed: 25406321]
7. Lim SY, Hong KH, Kim DI, Kwon H, Kim H. J Tunable heptamethineazo dye conjugate as a NIR fluorescent probe for the selective detection of mitochondrial glutathione over cysteine and homocysteine. *Journal of the American Chemical Society*. 2014; 136:7018–7025. [PubMed: 24754635]
8. Lim CS, Masanta G, Kim HJ, Han JH, Kim HM, Cho BR. Ratiometric detection of mitochondrial thiols with a two-photon fluorescent probe. *Journal of the American Chemical Society*. 2011; 133:11132–11135. [PubMed: 21718072]
9. Jiang X, Yu Y, Chen J, Zhao M, Chen H, Song X, Matzuk AJ, Carroll SL, Tan X, Sizovs A, Cheng N, Wang MC, Wang J. Quantitative imaging of glutathione in live cells using a reversible reaction-based ratiometric fluorescent probe. *ACS chemical biology*. 2015; 10:864–874. [PubMed: 25531746]
10. Wang, J., Jiang, X., Chen, J. Probes for quantitative imaging of thiols in various environments. WO2016025382. Priority date: 2014 Aug 09; Publication date: 2016 Feb 18
11. Jiang X, Chen J, Bajic A, Zhang C, Song X, Carroll SL, Cai Z, Tang M, Xue M, Cheng N, Schaaf CP, Li F, MacKenzie KR, Ferreon ACM, Xia F, Wang MC, Maletic-Savatic M, Wang J. Quantitative Real-Time Imaging of Glutathione. *Nature communications*. 2017; 8:16087–16098.

12. Umezawa K, Yoshida M, Kamiya M, Yamasoba T, Urano Y. Rational design of reversible fluorescent probes for live-cell imaging and quantification of fast glutathione dynamics. *Nature chemistry*. 2017; 9:279–286.
13. Liu Z, Zhou X, Miao Y, Hu Y, Kwon N, Wu X, Yoon J. A Reversible Fluorescent Probe for Real-time Quantitative Monitoring of Cellular Glutathione. *Angewandte Chemie*. 2017; 56:5812–5816. [PubMed: 28371097]
14. Smith RA, Porteous CM, Gane AM, Murphy MP. Delivery of bioactive molecules to mitochondria in vivo. *Proceedings of the National Academy of Sciences of the United States of America*. 2003; 100:5407–5412. [PubMed: 12697897]
15. Grimm JB, English BP, Chen J, Slaughter JP, Zhang Z, Revyakin A, Patel R, Macklin JJ, Normanno D, Singer RH, Lionnet T, Lavis LD. A general method to improve fluorophores for live-cell and single-molecule microscopy. *Nature methods*. 2015; 12:244–250. [PubMed: 25599551]
16. Dunn KW, Kamocka MM, McDonald JH. A practical guide to evaluating colocalization in biological microscopy. *American journal of physiology Cell physiology*. 2011; 300:C723–742. [PubMed: 21209361]
17. Nemoto S, Finkel T. Redox regulation of forkhead proteins through a p66shc-dependent signaling pathway. *Science*. 2002; 295:2450–2452. [PubMed: 11884717]



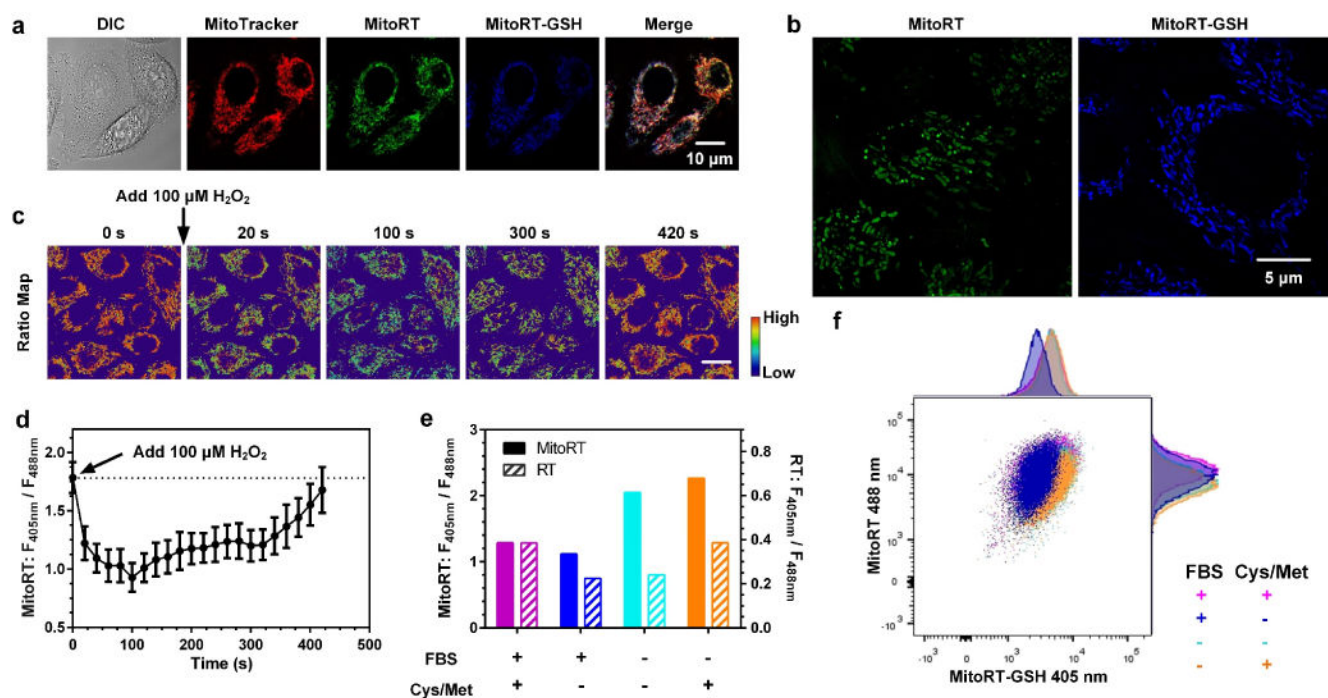
**Figure 1.**

The reversible Michael addition reaction between MitoRT and GSH. The function of each moiety in RT is highlighted (QY: quantum yield). The wiggled bond indicates either cis or trans configuration of the double bond.



**Figure 2.**

Characterization of reversible reaction-based mitochondria-specific glutathione probe MitoRT. **(a)** UV-vis (unshaded) and fluorescence (shaded) spectra of MitoRT (green) and MitoRT-GSH (blue), the GSH adduct. **(b)** Absorbance of equilibrated mixture between MitoRT and different concentrations of GSH (0, 0.16, 0.31, 0.63, 1.25, 2.5, 5, 10, 20, and 80 mM). **(c)** Sigmoidal relationship between normalized absorbance at 405 and 488 nm and GSH concentrations. **(d)** Linear relationship between  $(R-R_{\min})/(R_{\max}-R)$  and GSH concentrations.  $R = F_{405}/F_{488}$ .  $F_{405}$  and  $F_{488}$  are the fluorescence intensities for RT-GSH and RT, respectively.  $R_{\min}$  and  $R_{\max}$  are the  $R$  values at 0 and saturating (80 mM) GSH concentrations, respectively. **(e)** Reaction selectivity of MitoRT towards GSH. Fluorescence ratio  $F_{405}/F_{488}$  was measured after MitoRT probe equilibrated with physiological relevant concentrations of different compounds, including GSH (10 mM), glycine (10 mM), thiol containing compounds (100  $\mu\text{M}$ ) and reactive oxygen species (100  $\mu\text{M}$ ). **(f)** Forward reaction kinetics between MitoRT and GSH by mixing equal volumes of MitoRT (1  $\mu\text{M}$ ) and GSH (5 mM) solutions. The reaction was followed by monitoring the fluorescence changes of MitoRT-GSH ( $\lambda_{\text{ex}} = 395 \text{ nm}$ ). The kinetic profile is biphasic and the time to reach 90% of reaction completion is 26.5 seconds. **(g)** Reverse reaction kinetics between MitoRT and GSH by mixing equal volumes of a mixture of MitoRT (1  $\mu\text{M}$ ) and GSH (5 mM) solution and PBS. The reaction was followed by monitoring the fluorescence changes of MitoRT-GSH ( $\lambda_{\text{ex}} = 395 \text{ nm}$ ). The kinetic profile is biphasic and the time to reach 90% of reaction completion is 32.4 seconds. **(h)** Demonstration of reaction reversibility between MitoRT and GSH. To a MitoRT (1  $\mu\text{M}$ ) solution, GSH was added sequentially to reach final concentrations of 0.5, 1.0, 2.0 and 3.0 mM, followed by addition of 3.0 mM of *N*-methylmaleimide (NMM) to scavenge all the added GSH. The fluorescence was followed with an excitation wavelength of 405 nm and emission wavelength of 485 nm.

**Figure 3.**

MitoRT-based imaging of mitochondrial glutathione in living cells. **(a)** Confocal and ratiometric images of HeLa cells stained with MitoTracker and MitoRT. MitoRT and MitoRT-GSH are well colocalized with MitoTracker. Scale bar: 10  $\mu\text{m}$ . **(b)** Super-resolution image of MitoRT in living cells. Scale bar: 5  $\mu\text{m}$ . **(c–d)** Imaging of mGSH level fluctuations in HeLa cells upon treatment with  $\text{H}_2\text{O}_2$  (100  $\mu\text{M}$ ). Each data point represents the mean value of 30–75 areas from 8–15 cells analyzed from one representative time-lapsed imaging experiment. Error bars represent s.e.m. Scale bar: 20  $\mu\text{m}$ . **(e–f)** Comparison of cytosolic and mitochondrial GSH levels using RT and MitoRT, respectively, under FBS starvation conditions with and without sulfur containing amino acids in medium. Each bar represents the mean ratio of 16,000–24,000 cells; error bars represent s.e.m. and were too small to show clearly.